

# Microbial oxidation as a methane sink beneath the West Antarctic Ice Sheet

Alexander B. Michaud<sup>1\*†</sup>, John E. Dore<sup>1</sup>, Amanda M. Achberger<sup>2†</sup>, Brent C. Christner<sup>2,3</sup>, Andrew C. Mitchell<sup>4</sup>, Mark L. Skidmore<sup>5</sup>, Trista J. Vick-Majors<sup>1†</sup> and John C. Priscu<sup>1\*</sup>

**Aquatic habitats beneath ice masses contain active microbial ecosystems capable of cycling important greenhouse gases, such as methane (CH<sub>4</sub>). A large methane reservoir is thought to exist beneath the West Antarctic Ice Sheet, but its quantity, source and ultimate fate are poorly understood. For instance, O<sub>2</sub> supplied by basal melting should result in conditions favourable for aerobic methane oxidation. Here we use measurements of methane concentrations and stable isotope compositions along with genomic analyses to assess the sources and cycling of methane in Subglacial Lake Whillans (SLW) in West Antarctica. We show that sub-ice-sheet methane is produced through the biological reduction of CO<sub>2</sub> using H<sub>2</sub>. This methane pool is subsequently consumed by aerobic, bacterial methane oxidation at the SLW sediment–water interface. Bacterial oxidation consumes >99% of the methane and represents a significant methane sink, and source of biomass carbon and metabolic energy to the surficial SLW sediments. We conclude that aerobic methanotrophy may mitigate the release of methane to the atmosphere upon subglacial water drainage to ice sheet margins and during periods of deglaciation.**

Methane (CH<sub>4</sub>) is an important greenhouse gas that affects atmospheric chemistry and the radiative balance of Earth. Consequently, understanding its global sources, sinks, and feedbacks within the climate system is of considerable importance<sup>1</sup>. The primary pathway for biological CH<sub>4</sub> production in carbon-rich habitats (for example, bogs, wetlands) is the anaerobic fermentation of simple organic compounds by certain archaea (acetoclastic or methylotrophic methanogenesis<sup>2</sup>). An alternative microbial pathway to CH<sub>4</sub> production is the reduction of CO<sub>2</sub> coupled to the oxidation of H<sub>2</sub> (hydrogenotrophic methanogenesis), which is common in anoxic, low-sulfate environments such as the methanogenic zone within marine sediments<sup>2</sup>. Conversely, bacterial and archaeal oxidation of CH<sub>4</sub> (aerobic and anaerobic, respectively) to CO<sub>2</sub> is a major pathway that reduces net CH<sub>4</sub> release to the atmosphere<sup>3</sup>.

Anoxic habitats in sediments beneath the Antarctic ice sheet may be globally important sites of biological CH<sub>4</sub> production that could potentially add significant CH<sub>4</sub> to the atmosphere upon subglacial water drainage to the ice sheet margins or deglaciation<sup>4–6</sup>. However, due to release of oxygen into the subglacial environment from the overlying ice sheet through geothermal heat-induced melting<sup>7–9</sup>, aerobic methanotrophic activity can ultimately mitigate CH<sub>4</sub> release to the atmosphere. We present data on CH<sub>4</sub> concentration and stable isotopic composition, along with genomic data collected from Subglacial Lake Whillans (SLW), which lies ~800 m beneath the West Antarctic Ice Sheet (WAIS). Collectively, these data reveal the presence of an ecosystem supported, in part, by active microbial transformations of CH<sub>4</sub>.

## Quantity and source of sub-ice-sheet CH<sub>4</sub>

CH<sub>4</sub> concentration in SLW ranged from 0.024 μM in the lake water to 300 μM in the deepest (39 cm) sediment porewater sample (Fig. 1). Fick's first law was used to compute a flux of 6.8 ± 1.8 (mean ± SE) mmol CH<sub>4</sub> m<sup>-2</sup> yr<sup>-1</sup> into the surficial sediment (0–2 cm) of SLW using the concentration gradient in the top 15 cm of sediment and the associated error of the concentration gradient, which includes any potential sampling artefacts. CH<sub>4</sub> in the SLW sediment had an average δ<sup>13</sup>C–CH<sub>4</sub> value of –74.7‰ (range: –77.1 to –70.1‰) (Fig. 1) and, together with δD–CH<sub>4</sub> values (range: –247.6 to –239.3‰), reveals that SLW CH<sub>4</sub> is probably produced by hydrogenotrophic methanogenesis<sup>10</sup> (Fig. 2). This conclusion contrasts with previous models suggesting that potential CH<sub>4</sub> reservoirs beneath the WAIS would be largely formed through acetoclastic methanogenesis<sup>4</sup>. Hydrogenotrophic methanogenesis is common in marine sediments and other environments with low concentrations of old organic carbon, supporting our results from SLW, which also has low organic carbon and acetate (2–14 μM) relative to environments with active acetoclastic methanogenesis<sup>10–13</sup> (Supplementary Fig. 1). CO<sub>2</sub> for hydrogenotrophic methanogenesis can be supplied from microbial respiration or bicarbonate in sediment porewater (2–6 mM; ref. 14), and hydrogen can be generated abiotically from glacially crushed siliceous bedrock, radiolysis of water, hydrothermal input, or biologically via fermentation<sup>2,8,15,16</sup>. Attempts to amplify a marker gene for methanogenic archaea (*mcrA*)<sup>17,18</sup> from the 0–2, 4–6, 18–20 and 34–36 cm depth intervals within the SLW sediment core were unsuccessful, implying that the abundance of methanogenic archaea was low or below detection.

<sup>1</sup>Department of Land Resources and Environmental Sciences, Montana State University, Bozeman, Montana 59717, USA. <sup>2</sup>Department of Biological Sciences, Louisiana State University, Baton Rouge, Louisiana 70803, USA. <sup>3</sup>Department of Microbiology and Cell Science, University of Florida, Gainesville, Florida 32611, USA. <sup>4</sup>Department of Geography and Earth Sciences, Aberystwyth University, Aberystwyth SY23 3DB, UK. <sup>5</sup>Department of Earth Sciences, Montana State University, Bozeman, Montana 59717, USA. <sup>†</sup>Present addresses: Center for Geomicrobiology, Department of Bioscience, Aarhus University, 8000 Aarhus C, Denmark (A.B.M.); Department of Oceanography, Texas A&M University, College Station, Texas 77840, USA (A.M.A.); Département des Sciences Biologiques, Université du Québec à Montréal, Case Postale 8888, Succursale Centre-Ville, Montréal, Quebec H3C 3P8, Canada (T.J.V.-M.).

\*e-mail: a.b.michaud@gmail.com; jpriscu@montana.edu

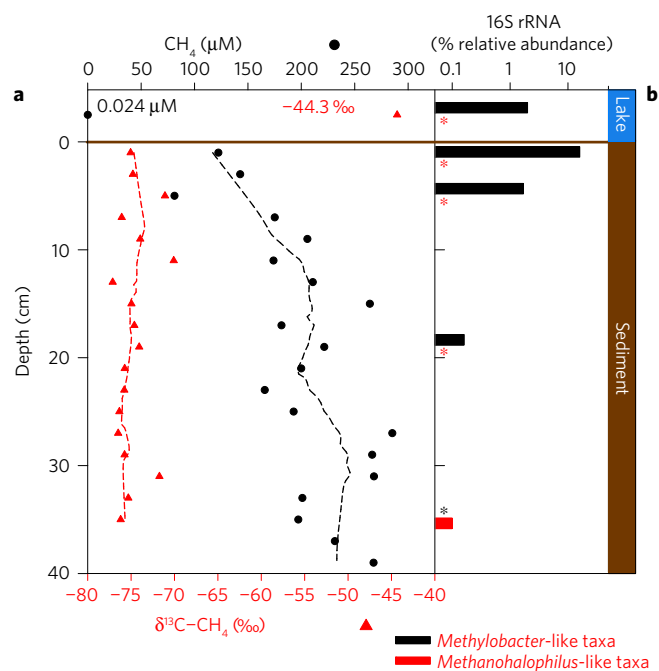


**Figure 1 |** SLW water column and sediment profiles of CH<sub>4</sub> concentration, stable isotope composition and abundance of active methane oxidizing and methanogenic taxa. **a**, CH<sub>4</sub> concentration and δ<sup>13</sup>C-CH<sub>4</sub> values. Dashed lines indicate running averages using a Loess smoothing function. SLW water column values for CH<sub>4</sub> concentration and stable isotope values are displayed next to points. **b**, Percentage relative abundance of known CH<sub>4</sub> oxidizing and methanogenic bacterial and archaeal taxa, respectively, from the community analysis of 16S rRNA molecules (note log scale; modified from ref. 21). Asterisks indicate that methanogenic (red) and methanotrophic (black) genera were not detected.

A community analysis of 16S rRNA molecules, which indicates the potentially active fraction of the microbial community<sup>19,20</sup>, showed relatives of methanogenic species (that is, *Methanohalophilus levihalophilus*) were rare members (0.1%) of the active sediment community at 35 cm depth (Fig. 1b)<sup>21</sup>. The most parsimonious explanation for our concentration profile and molecular microbiological results is the presence of a contemporary or relict CH<sub>4</sub> source that originates from depths below our deepest sample and diffuses towards an aerobic methanotrophic sink at the sediment–water interface.

**Active aerobic methanotrophy**

The low water column CH<sub>4</sub> concentration, relative to the sediment porewater, and the decrease in CH<sub>4</sub> concentration in the upper ~16 cm of sediment indicate that CH<sub>4</sub> oxidation consumes almost all (>99%) of the upwardly diffusing sedimentary CH<sub>4</sub> (Fig. 1a). The four order of magnitude decrease in CH<sub>4</sub> concentration from the surficial sediments to the water column corresponds with a large, positive shift (30.7‰) in the δ<sup>13</sup>C-CH<sub>4</sub> values (Fig. 1a). We used the Rayleigh distillation model to calculate a kinetic isotope fractionation factor (KIFF) of α = 1.004 associated with the CH<sub>4</sub> oxidation process<sup>22</sup>. This model assumes a closed system (that is, no other inputs of CH<sub>4</sub> and measured isotope values are not affected by mixing) and that the only sink for sedimentary CH<sub>4</sub> is bacterial oxidation. The KIFF calculated for CH<sub>4</sub> oxidation in SLW is within the lower range of those derived from laboratory cultures, but is similar to estimates from field measurements made in cold, marine habitats (α = 1.003–1.035; refs 22,23). The observed fractionation in SLW is consistent with near-complete removal of upwardly diffusing sedimentary CH<sub>4</sub> by aerobic CH<sub>4</sub> oxidizing bacteria<sup>23</sup>.

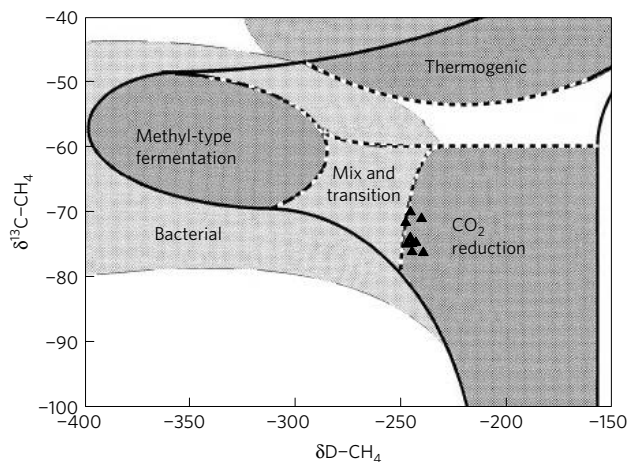


**Figure 2 |** CH<sub>4</sub> stable isotope biplot for nine depths of the SLW sediment porewater (black triangles). The shaded areas delineate microbial and thermogenic endmembers as well as regions of mixed sources (endmember fields modified from ref. 10). δ<sup>13</sup>C-CH<sub>4</sub> values in this plot are the same as Fig. 1a.

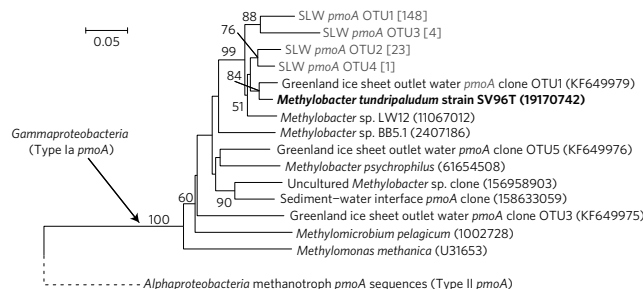


**Figure 3 |** Neighbour-joining phylogenetic tree of SLW *pmoA* DNA sequences. *pmoA* sequences from SLW water column and sediment are highlighted in grey and brackets indicate the number of sequenced clones within each operational taxonomic unit (OTU) with sequence accession numbers shown in parentheses. All solid line branches are *pmoA* sequences of the *Gammaproteobacteria* type Ia group, including *Methylobacter tundripaludum* (bold), an active and abundant member of the SLW community<sup>1,17</sup>. Bootstrap support is displayed at branch points (%; 1,000 replications), with values >50% shown. Branch lengths are measured in number of substitutions per site. The scale bar represents 0.05 substitutions per site.

We amplified the β-subunit of the particulate methane monooxygenase gene (*pmoA*) found in aerobic CH<sub>4</sub> oxidizing bacteria to further evaluate the functional potential for CH<sub>4</sub> oxidation. Results revealed that *pmoA* was detectable in the water column and the upper 16 cm of sediment, but not in deeper layers of the core. The presence of *pmoA* genes is consistent with the measured O<sub>2</sub> concentration of 71.9 µM, in SLW lake waters<sup>1</sup>, and redox-sensitive trace metal abundance in the sediment core that implies the presence of O<sub>2</sub> to a depth of ~16 cm (ref. 14). Thus, the functional potential for aerobic methanotrophy (*pmoA* gene presence) occurs where both CH<sub>4</sub> and O<sub>2</sub> are available. SLW *pmoA* sequences were similar (>87% DNA similarity) to *Methylobacter tundripaludum*, an aerobic CH<sub>4</sub> oxidizing bacterium (Fig. 3). *M. tundripaludum* was also the closest described and cultured phylogenetic relative (99% rDNA gene sequence similarity) to the putative CH<sub>4</sub> oxidizing taxa recovered from 16S rDNA gene sequence analysis of the SLW microbial community (Fig. 3; OTU 000112; refs 7,21). The *pmoA* sequences present in SLW were related to *pmoA* sequences collected from an active CH<sub>4</sub> oxidizing environment at the margin of the Greenland Ice Sheet

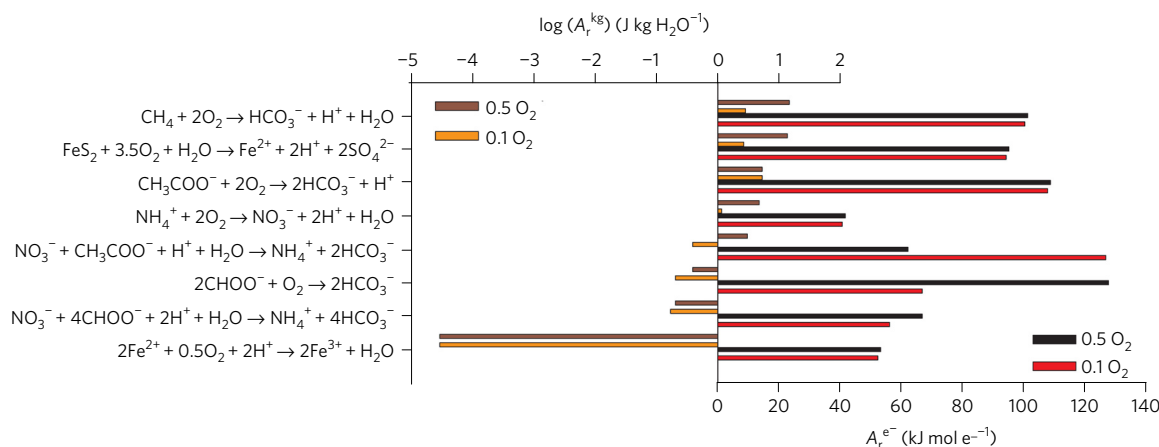


**Figure 4 | Chemical affinity calculations for the SLW surficial (0–2 cm) sediment.** Results are presented in energy density of joules per kg of water ( $\text{J kg H}_2\text{O}^{-1}$ ; top axis in log scale) and kilojoules per mole of electron transferred ( $\text{kJ mol e}^{-1}$ ; bottom axis) at 50% (0.5) and 10% (0.1) of the SLW lake water  $\text{O}_2$  concentration for eight environmentally relevant biochemical reactions.

(Fig. 3)<sup>5</sup>. Although the *pmoA* primer set we used was designed to detect a wide diversity of methanotrophs<sup>24</sup>, additional putative methanotrophic genera were detected in the 16S rDNA and rRNA community analysis (Supplementary Fig. 2), but these genera were at least one order of magnitude less abundant than *M. tundripaludum*.

Aerobic  $\text{CH}_4$  oxidizing bacteria are typically members of the *Gammaproteobacteria* and *Alphaproteobacteria*<sup>25</sup> and further classified into different types based on the substrate affinity of their methane monooxygenase enzyme<sup>25</sup>. Type Ia *Gammaproteobacteria* methanotrophs have methane monooxygenase enzymes with low affinity for  $\text{CH}_4$  while type II *Alphaproteobacteria* have enzymes with a high affinity for  $\text{CH}_4$  (ref. 26). These type Ia *Gammaproteobacteria* methanotrophs, particularly *Methylobacter* sp., dominate the active fraction of methanotroph populations in freshwater environments that have high  $\text{CH}_4$  ( $\mu\text{M}$ – $\text{mM}$ ) concentrations and strong  $\text{CH}_4$  sources<sup>25,26</sup>. *M. tundripaludum* possesses a low-affinity (type Ia) methane monooxygenase enzyme, is known to be cold-adapted<sup>24,26</sup>, has been shown to be active at the Greenland Ice Sheet margin<sup>5</sup> and is responsible for significant  $\text{CH}_4$  consumption in a variety of other Arctic habitats<sup>27–29</sup>. Both the low  $\text{CH}_4$  affinity and temperature adaptation of the type Ia *Gammaproteobacteria* particulate methane monooxygenase enzyme reflect the conditions measured in SLW surficial sediments ( $-0.5^\circ\text{C}$  and 0.1 to 0.3  $\text{mM CH}_4$ ; Fig. 1)<sup>9</sup>. Indeed, a community analysis of 16S rRNA molecules showed *M. tundripaludum* and other methanotrophic taxa were abundant ( $\geq 1.0\%$ ) in the water column and upper sediments (0–6 cm), with their greatest relative abundance in the surficial sediments (16%; Fig. 1b; Supplementary Fig. 2)<sup>21</sup>. These molecular data, based on *pmoA* gene sequences and 16S rRNA molecules, indicate that methanotrophs related to *M. tundripaludum* are abundant and potentially metabolically active near the SLW sediment–water interface, where geochemical data indicate peak methane oxidation.

### The role of $\text{CH}_4$ in the subglacial ecosystem

We computed chemical affinity ( $A_r$ ) for the surficial (0–2 cm) sediment layer to estimate the available biochemical energy from  $\text{CH}_4$  oxidation compared to other potential metabolic reactions<sup>30,31</sup> (Fig. 4).  $\text{O}_2$  concentration data in the surficial sediment layer are not available, so biochemical reactions were modelled at half (36.5  $\mu\text{M}$ ) and one-tenth (7.3  $\mu\text{M}$ ) of the average SLW water column  $\text{O}_2$  concentration. These modelled  $\text{O}_2$  concentrations are reasonable given the evidence for  $\text{O}_2$  penetration to  $\sim 16$  cm (ref. 14). Although pyrite and ammonium oxidation are predicted to yield the greatest metabolic energy in the water column<sup>32</sup>, aerobic  $\text{CH}_4$  oxidation is the most exergonic biochemical pathway in the surficial sediment

despite the modelled tenfold reduction in  $\text{O}_2$  concentration relative to lake water ( $A_r^-$ : 99.9  $\text{kJ mol e}^{-1}$ ;  $A_r^{\text{kg}}$ : 2.84  $\text{J kg H}_2\text{O}^{-1}$ ) (Fig. 4). The microbial community composition reflects the chemical affinity calculations such that iron, sulfide and ammonium oxidizing taxa are abundant in the water column<sup>21,32</sup> and aerobic methane oxidizing taxa are abundant and active in the surficial sediment (Fig. 1). These chemical affinity calculations corroborate the molecular and geochemical data by showing sufficient biochemical energy is present in the SLW surficial sediment to support the abundant methanotroph population (Fig. 4).

We modelled the rate of biological  $\text{CH}_4$  consumption in SLW as:

$$\frac{dC}{dt} = (F_{\text{diff}} \times A) - (R \times V) \quad (1)$$

where  $dC/dt$  is the change in  $\text{CH}_4$  concentration over time,  $F_{\text{diff}}$  is the diffusional flux into the 0–2 cm surficial sediment,  $A$  is the area of SLW,  $R$  is the rate of  $\text{CH}_4$  consumption, and  $V$  is volume of SLW plus the porewater surficial sediment. Assuming steady-state conditions (that is,  $dC/dt = 0$ ), equation (1) can be rewritten as:

$$R = \frac{F_{\text{diff}}}{H_L + (H_{\text{SS}} \times \varphi)} \quad (2)$$

where  $H_L$  and  $H_{\text{SS}}$  are the height of the lake and surficial (0–2 cm) sediments, respectively, and  $\varphi$  is the sediment porosity.  $R$  equates to  $3.0 \pm 0.8 \text{ mmol CH}_4 \text{ m}^{-3} \text{ yr}^{-1}$ . The rate of  $\text{CH}_4$  removal ( $R$ ) is the sum of both  $\text{CH}_4$  oxidation ( $R_{\text{ox}}$ ) and incorporation of  $\text{CH}_4$  as a carbon source ( $R_{\text{incorp}}$ ) for microbial biomass synthesis. Using the total  $\text{CH}_4$  removal rate ( $R$ ), together with the average fraction of  $\text{CH}_4$  ( $\sim 0.5$ ) partitioned to biomass formation for type I methanotrophs<sup>33</sup>, reveals that methanotrophs may oxidize  $1.5 \text{ mmol CH}_4 \text{ m}^{-3} \text{ yr}^{-1}$  to  $\text{CO}_2$  ( $R_{\text{ox}}$ ) and assimilate  $1.5 \text{ mmol CH}_4 \text{ m}^{-3} \text{ yr}^{-1}$  ( $R_{\text{incorp}}$ ) as a biosynthetic carbon source (Supplementary Table 1). Given 0.5 as a biomass partitioning factor, the rate of aerobic  $\text{CH}_4$  oxidation would be 10- to 100-fold lower than aerobic  $\text{CH}_4$  oxidation measured in cold ( $\sim 4^\circ\text{C}$ ), surficial marine sediments and deep sea,  $\text{CH}_4$  seeps<sup>34,35</sup>. The biomass partitioning factor can vary from 0.06 to 0.7 in lakes with active methanotrophy<sup>36</sup>. When we account for this potential variability in the biomass partitioning factor and the uncertainty in the  $\text{CH}_4$  flux,  $R_{\text{ox}}$  and  $R_{\text{incorp}}$  vary by an order of magnitude; the range of  $R_{\text{incorp}}$  is 0.14–3.0  $\text{mmol CH}_4 \text{ m}^{-3} \text{ yr}^{-1}$  and  $R_{\text{ox}}$  is 0.52–3.6  $\text{mmol CH}_4 \text{ m}^{-3} \text{ yr}^{-1}$  (Supplementary Table 1). It is important to note that  $R_{\text{ox}}$  and  $R_{\text{incorp}}$  are inversely related (Supplementary Table 1). Although the overall rate of oxidation

may be low compared to marine sediment methanotrophy, if the formation of biomass due to CH<sub>4</sub> oxidation occurred solely in the surficial SLW sediment porewaters, where molecular data indicate peak active methanotroph abundance (Fig. 1b), the biosynthetic rate would be 26.2 ng C (L porewater)<sup>-1</sup> d<sup>-1</sup> (range: 2.3–51 ng C (L porewater)<sup>-1</sup> d<sup>-1</sup>; Supplementary Table 1). This modelled biomass C production rate via sedimentary methanotrophy is nearly equivalent (80%; range: 7–155%) to measured rates of chemoautotrophic biomass C production (32.9 ng C L<sup>-1</sup> d<sup>-1</sup>) within the SLW water column<sup>7</sup>. These results indicate that CH<sub>4</sub>, as modelled, is an important carbon and energy source for the SLW sediment microbial community.

The O<sub>2</sub> demand derived from the modelled CH<sub>4</sub> removal rate (R) is 6.1 × 10<sup>5</sup> mol O<sub>2</sub> yr<sup>-1</sup>, using 0.5 as the biomass partitioning factor. Methanotrophy in SLW is responsible for consuming ~16% (range: 10–24%; Supplementary Table 1) of the O<sub>2</sub> supply to the SLW ecosystem<sup>32</sup>. Thus, the impact of oxygen demand due to CH<sub>4</sub> oxidation in the SLW ecosystem depends on the balance between methanotroph growth and energy requirements. Despite a potentially large range in the biomass partitioning factor, these calculations show that O<sub>2</sub> released from basal melting of the overlying ice sheet fuels an abundant and active population of methanotrophs in the lake. Saturated sediments at SLW are similar in nature to those found beneath other ice streams of the Siple coast region (for example, ref. 8) and basal ice melt is extensive beneath the WAIS<sup>37,38</sup>, which may produce extensive oxic subglacial aquatic habitats, conducive to cosmopolitan populations of methanotrophs that convert CH<sub>4</sub> to CO<sub>2</sub> and biomass.

Our data reveal that hydrogenotrophic methanogenesis is the main pathway of CH<sub>4</sub> formation beneath SLW and that CH<sub>4</sub> is utilized by aerobic methanotrophic bacteria. Contrary to previous predictions which suggested the potential significance of subglacial CH<sub>4</sub> fluxes to the atmosphere (for example, ref. 4), our CH<sub>4</sub> measurements and flux calculations show that aerobic methanotrophic bacteria in SLW convert most (>99%) of the sedimentary CH<sub>4</sub> efflux to CO<sub>2</sub> and biomass. The bacterial conversion of CH<sub>4</sub> to CO<sub>2</sub> beneath the WAIS reduces the warming potential of subglacial gases<sup>39</sup> that may be released to downstream ice sheet margin environments and to the atmosphere during episodes of ice sheet retreat. Given the potential for widespread hydrogenotrophic CH<sub>4</sub> production in sediments beneath ice sheets, such as the WAIS, and the release of O<sub>2</sub> due to melting at the ice sheet base<sup>9,37,38</sup>, biological transformations of CH<sub>4</sub> may be significant for the functioning and persistence of deep microbial life and biogeochemical processes in Antarctic sub-ice environments.

## Methods

Methods, including statements of data availability and any associated accession codes and references, are available in the [online version of this paper](#).

Received 17 March 2017; accepted 26 June 2017;  
published online 31 July 2017

## References

- Kirschke, S. *et al.* Three decades of global methane sources and sinks. *Nat. Geosci.* **6**, 813–823 (2013).
- Thauer, R. K., Kaster, A.-K., Seedorf, H., Buckel, W. & Hedderich, R. Methanogenic archaea: ecologically relevant differences in energy conservation. *Nat. Rev. Microbiol.* **6**, 579–591 (2008).
- Conrad, R. The global methane cycle: recent advances in understanding the microbial processes involved. *Environ. Microbiol. Rep.* **1**, 285–292 (2009).
- Wadham, J. L. *et al.* Potential methane reservoirs beneath Antarctica. *Nature* **488**, 633–637 (2012).
- Dieser, M. *et al.* Molecular and biogeochemical evidence for methane cycling beneath the western margin of the Greenland Ice Sheet. *ISME J.* **8**, 2305–2316 (2014).
- Wadham, J. L. *et al.* The potential role of the Antarctic Ice Sheet in global biogeochemical cycles. *Earth Environ. Sci. Trans. R. Soc. Edinburgh* **104**, 55–67 (2013).
- Christner, B. C. *et al.* A microbial ecosystem beneath the West Antarctic Ice Sheet. *Nature* **512**, 310–313 (2014).
- Skidmore, M. in *Antarctic Subglacial Environments, Geophysical Monograph Series* (eds Siegert, M. J., Kennicutt II, M. C. & Bindschandler, R. A.) 61–81 (American Geophysical Union, 2011).
- Fisher, A. T., Mankoff, K. D., Tulaczyk, S. M. & Tyler, S. W. High geothermal heat flux measured below the West Antarctic Ice Sheet. *Sci. Rep.* **1**, e1500093 (2015).
- Whiticar, M. J. Carbon and hydrogen isotope systematics of bacterial formation and oxidation of methane. *Chem. Geol.* **161**, 291–314 (1999).
- Coleman, D. D., Liu, C.-L. & Riley, K. M. Microbial methane in the shallow Paleozoic sediments and glacial deposits of Illinois, USA. *Chem. Geol.* **71**, 23–40 (1988).
- Conrad, R. in *Advances in Agronomy* (ed. Sparks, S.) 1–63 (Elsevier, 2007).
- Schoell, M. Multiple origins of methane in the Earth. *Chem. Geol.* **71**, 1–10 (1988).
- Michaud, A. B. *et al.* Solute sources and geochemical processes in Subglacial Lake Whillans, West Antarctica. *Geology* **44**, 347–350 (2016).
- Telling, J. *et al.* Rock comminution as a source of hydrogen for subglacial ecosystems. *Nat. Geosci.* **8**, 851–855 (2015).
- Lin, L.-H., Slater, G. F., Sherwood Lollar, B., Lacrampe-Couloume, G. & Onstott, T. C. The yield and isotopic composition of radiolytic H<sub>2</sub>, a potential energy source for the deep subsurface biosphere. *Geochim. Cosmochim. Acta* **69**, 893–903 (2005).
- Matheus Carnevali, P. B. *et al.* Methane sources in arctic thermokarst lake sediments on the North Slope of Alaska. *Geobiology* **13**, 181–197 (2015).
- Lever, M. A. *et al.* Evidence for microbial carbon and sulfur cycling in deeply buried ridge flank basalt. *Science* **339**, 1305–1308 (2013).
- Blazewicz, S. J., Barnard, R. L., Daly, R. A. & Firestone, M. K. Evaluating rRNA as an indicator of microbial activity in environmental communities: limitations and uses. *ISME J.* **7**, 2061–2068 (2013).
- Jones, S. E. & Lennon, J. T. Dormancy contributes to the maintenance of microbial diversity. *Proc. Natl Acad. Sci. USA* **107**, 5881–5886 (2010).
- Achberger, A. M. *et al.* Microbial community structure of Subglacial Lake Whillans, West Antarctica. *Front. Microbiol.* **7**, 1457 (2016).
- Grant, N. J. & Whiticar, M. J. Stable carbon isotopic evidence for methane oxidation in plumes above Hydrate Ridge, Cascadia Oregon Margin. *Global Biogeochem. Cycles* **16**, 1124 (2002).
- Coleman, D. D., Risatti, J. B. & Schoell, M. Fractionation of carbon and hydrogen isotopes by methane-oxidizing bacteria. *Geochim. Cosmochim. Acta* **45**, 1033–1037 (1981).
- McDonald, I. R., Bodrossy, L., Chen, Y. & Murrell, J. C. Molecular ecology techniques for the study of aerobic methanotrophs. *Appl. Environ. Microbiol.* **74**, 1305–1315 (2008).
- Knief, C. Diversity and habitat preferences of cultivated and uncultivated aerobic methanotrophic bacteria evaluated based on pmoA as molecular marker. *Front. Microbiol.* **6**, 1346 (2015).
- Ho, A. *et al.* Conceptualizing functional traits and ecological characteristics of methane-oxidizing bacteria as life strategies. *Environ. Microbiol. Rep.* **5**, 335–345 (2013).
- Martineau, C., Whyte, L. G. & Greer, C. W. Stable isotope probing analysis of the diversity and activity of methanotrophic bacteria in soils from the Canadian high Arctic. *Appl. Environ. Microbiol.* **76**, 5773–5784 (2010).
- Graef, C., Hestnes, A. G., Svenning, M. M. & Frenzel, P. The active methanotrophic community in a wetland from the High Arctic. *Environ. Microbiol. Rep.* **3**, 466–472 (2011).
- He, R. *et al.* Shifts in identity and activity of methanotrophs in Arctic lake sediments in response to temperature changes. *Appl. Environ. Microbiol.* **78**, 4715–4723 (2012).
- Shock, E. L. *et al.* Quantifying inorganic sources of geochemical energy in hydrothermal ecosystems, Yellowstone National Park, USA. *Geochim. Cosmochim. Acta* **74**, 4005–4043 (2010).
- Amend, J. P. & Shock, E. L. Energetics of overall metabolic reactions of thermophilic and hyperthermophilic Archaea and Bacteria. *FEMS Microbiol. Rev.* **25**, 175–243 (2001).
- Vick-Majors, T. J. *et al.* Physiological ecology of microorganisms in Subglacial Lake Whillans. *Front. Microbiol.* **7**, 1705 (2016).
- Trimmer, M. *et al.* Riverbed methanotrophy sustained by high carbon conversion efficiency. *ISME J.* **9**, 2304–2314 (2015).
- Iversen, N. & Blackburn, T. H. Seasonal rates of methane oxidation in anoxic marine sediments. *Appl. Environ. Microbiol.* **41**, 1295–1300 (1981).
- Marlow, J. J. *et al.* Carbonate-hosted methanotrophy represents an unrecognized methane sink in the deep sea. *Nat. Commun.* **5**, 5094 (2014).

36. Bastviken, D., Ejlertsson, J., Sundh, I. & Tranvik, L. Methane as a source of carbon and energy for lake pelagic food webs. *Ecology* **84**, 969–981 (2003).
37. Lough, A. C. *et al.* Seismic detection of an active subglacial magmatic complex in Marie Byrd Land, Antarctica. *Nat. Geosci.* **6**, 1031–1035 (2013).
38. Beem, L. H., Jezek, K. C. & Van Der Veen, C. J. Basal melt rates beneath Whillans Ice Stream, West Antarctica. *J. Glaciol.* **56**, 647–654 (2010).
39. Yvon-Durocher, G. *et al.* Methane fluxes show consistent temperature dependence across microbial to ecosystem scales. *Nature* **507**, 488–491 (2014).

### Acknowledgements

This study was funded by National Science Foundation – Division of Polar Programs grants (0838933, 1346250, 1439774 to J.C.P.; 0838941 to B.C.C.) awarded as part of the Whillans Ice Stream Subglacial Access Research Drilling (WISSARD) project. We thank the WISSARD Science Team (see <http://wissard.org> for the full list of team members) for their assistance in expedition planning and with collecting and processing samples. Partial support was provided by graduate fellowships from the NSF-IGERT Program (0654336), Montana Space Grant Consortium and NSF-Center for Dark Energy Biosphere Investigations (A.B.M.); a dissertation grant from the American Association of University Women (T.J.V.-M.); a NSF-Graduate Research Fellowship (A.M.A.); and a Sêr Cymru National Research Network for Low Carbon, Energy and the Environment Grant from the Welsh Government and Higher Education Funding Council for Wales (A.C.M.). We thank R. Scherer and R. Powell for sediment cores. B.B. Jørgensen, M. A. Lever and

S. Nielsen provided support and assistance with DNA extraction and *pmoA/mcrA* amplification. Logistics were conducted by the 139th Expeditionary Airlift Squadron of the New York Air National Guard, Kenn Borek Air, and Antarctic Support Contractor, managed by Lockheed-Martin. Hot-water drill support was provided by University of Nebraska-Lincoln and directed by F. Rack and D. Duling (chief driller). D. Blythe, J. Burnett, C. Carpenter, D. Gibson, J. Lemery, A. Melby and G. Roberts provided drill support at SLW. This is C-DEBI contribution #371.

### Author contributions

A.B.M., J.E.D., T.J.V.-M., J.C.P. and M.L.S. wrote the manuscript. A.B.M., J.E.D., M.L.S. and T.J.V.-M. conducted and analysed methane concentration and isotopic data. A.M.A., A.B.M. and B.C.C. processed, analysed and interpreted the molecular data. A.C.M. conducted thermodynamic calculations. All authors contributed to the study design, collection of samples and approved the final draft of the manuscript.

### Additional information

Supplementary information is available in the [online version of the paper](#). Reprints and permissions information is available online at [www.nature.com/reprints](http://www.nature.com/reprints). Publisher's note: Springer Nature remains neutral with regard to jurisdictional claims in published maps and institutional affiliations. Correspondence and requests for materials should be addressed to A.B.M. or J.C.P.

### Competing financial interests

The authors declare no competing financial interests.

## Methods

**Sample collection.** We used a microbiologically clean hot-water drill to directly sample the water column and the upper 40 cm of sediment of Subglacial Lake Whillans (SLW; 84.240° S, 153.694° W) to assess the CH<sub>4</sub> dynamics<sup>40,41</sup>. SLW water column and sediment were sampled through a 800-m-deep, ~0.6-m-diameter borehole on 30 January 2013. The clean access hot-water drill system has been shown to reduce cell concentrations within the drilling water to <100 cell ml<sup>-1</sup>, which is acceptable based on the predicted cell concentration in the lake water and the National Research Council 2007 report on subglacial lake access<sup>40,42</sup>. The 2.2-m-deep SLW water column was sampled with a 10 l Niskin bottle, suspended microbial cells were concentrated using an *in situ* water filtration system, and surficial sediments were collected with a gravity multicorer (60 cm long × 6 cm diameter). For complete drilling and sampling details see ref. 40,41.

**Geochemical analysis.** Sediment from a gravity core (MC-2A) was sampled every 2 cm by extrusion and subsampling of each newly exposed layer. Sediment subsamples for methane (CH<sub>4</sub>) were collected using a sterile cut-off 5 ml syringe and immediately placed into 20 ml sterile serum vials and stoppered with a sterile butyl rubber stopper, then crimped with an aluminium cap. Three empty vials were sealed in the field to capture atmospheric air as procedural blanks. Ten ml of 2.5% NaOH was added by sterile syringe to each sample vial and the three blanks, stopping biological activity and creating a pressurized headspace within each vial<sup>43</sup>. A CH<sub>4</sub> sample from the SLW water column was collected from cast 1 from a Niskin bottle by placing the tube to the bottom of the serum vial and filling from top to bottom. The water sample was fixed with Lugol's solution to prevent biological activity. All vials were stored inverted at 4 °C for transport back to Montana State University (MSU) for CH<sub>4</sub> quantification. Headspace CH<sub>4</sub> was quantified on a Hewlett-Packard 5890 Series II gas chromatograph (GC) equipped with a flame ionization detector (FID) with a detection limit of 3 nM for water column samples and 190 nM for the sediment samples. Headspace gas was introduced to the GC using a 10-port injection valve configured for back flushing of a precolumn (25 cm × 0.32 cm OD, packed with Porapak-T 80/100 mesh) to prevent water vapour from reaching the analytical columns. The vial overpressure was used to flush and fill a 1 cm<sup>3</sup> sample loop using a syringe needle inlet; measured laboratory air temperature and pressure were used to calculate the total moles of gas contained within the loop, assuming gas ideality. Gases were separated on two analytical columns in series (both 183 cm × 0.32 cm OD, packed with Chromosorb 102 80/100 mesh and Porapak-Q 80/100 mesh, respectively). The columns were maintained at 55 °C and the FID at 240 °C. The carrier gas was an ultra-high purity N<sub>2</sub>, which was further purified through Molecular Sieve 5A, activated charcoal and an O<sub>2</sub> scrubber. The carrier flow was 30 ml min<sup>-1</sup>; under these conditions, CH<sub>4</sub> eluted to the FID at 1.97 min. Instrument calibration was performed using certified 500 and 51 ppmv CH<sub>4</sub> in air standards (Air Liquide; ±1% accuracy), and volumetric dilutions thereof into carrier N<sub>2</sub>. Dissolved CH<sub>4</sub> concentrations were calculated using Henry's law based on measured headspace mole fractions and Bunsen solubility coefficients estimated from temperature and sample salinity (including added NaOH) as parameterized by ref. 44. Porewater volumes were determined from mass loss after drying the sediment at 95 °C until the mass stopped decreasing (~24 h), and dry sediment volume was similarly determined assuming a density of 2.60 g cm<sup>-3</sup> for the sedimentary particles<sup>45</sup>. The total volume of the vials was determined weighing the vials with sediment and NaOH fixative, then completely filling the headspace with deionized water and weighing again. The headspace volume was determined by difference. The extent of pressurization of the headspace was determined from total headspace volume and the volume of NaOH solution added. The total CH<sub>4</sub> within each vial, after correction for the small amount of CH<sub>4</sub> present in the headspace air when originally sealed (characterized by the blank vials), was then used to determine the initial CH<sub>4</sub> concentration of the porewater.

Gravity core MC-3A was collected from SLW, capped and immediately frozen (−20 °C). The frozen core was returned to MSU and thawed at 4 °C overnight in a class 1,000 clean, cold room in the MSU SubZero Science and Engineering Facility. The core was extruded and cut every 2 cm, and sediment for CH<sub>4</sub> stable isotope analysis was subsampled and fixed using the same method as for CH<sub>4</sub> concentration analysis from MC-2A described above. One ml of room-temperature headspace gas from the fixed sediment vials was transferred to a gas-tight laminated foil bag using a gas-tight, glass syringe and diluted 1:100 with CH<sub>4</sub>-free (zero grade) air. The bag was connected to the inlet of a Picarro G2201-*i* Cavity Ring-Down Spectrometer (CRDS) specific for high-precision concentration and δ<sup>13</sup>C analyses of CH<sub>4</sub>. Sample was introduced to the instrument at a flow rate of 100 ml min<sup>-1</sup>; δ<sup>13</sup>C–CH<sub>4</sub> values were determined using factory calibrations and were averaged over ≥30 s of 1 Hz measurements. Between samples, atmospheric air was measured for at least 5 min to ensure lack of instrument drift. The δD–CH<sub>4</sub> values were measured at the University of California Davis Stable Isotope Facility (UCD-SIF) using a PreCon concentration system (ThermoScientific) in line with a Delta V plus isotope ratio mass spectrometer (ThermoScientific)<sup>46</sup>. Two δ<sup>13</sup>C–CH<sub>4</sub> samples (MC-3A samples from 18 to 20 cm and 34–36 cm depths) were also run at

UCD-SIF to compare their independent results with our values obtained on the Picarro CRDS. There was a <4% difference in the δ<sup>13</sup>C–CH<sub>4</sub> values reported from the two methods. The carbon and hydrogen stable isotope ratios are reported in δ-notation (δ<sup>13</sup>C, δD) with respect to Vienna Pee Dee Belemnite (VPDB) and Vienna Standard Mean Ocean Water (VSMOW) standards, respectively. The running average (with depth) of the CH<sub>4</sub> concentration and isotope values was calculated in SigmaPlot v. 11 using a locally estimated scatterplot smoothing (Loess) function with smoothing parameters set to first-degree polynomial and a sampling frequency of 0.45, which determines the number of local data points used in the weighted regression carried out by the Loess smoothing function.

Sediments used for dissolved NH<sub>4</sub><sup>+</sup> concentration measurements were collected from MC-3A (ref. 47). The sediment was transferred to acid-washed (10% HCl), ultra-pure water-rinsed (6×), combusted (4 h at 450 °C) glass vials with polytetrafluoroethylene lined caps, frozen at −20 °C and thawed prior to analysis. Sediments were transferred from the glass vials to acid-washed and ultra-pure water-rinsed 50 ml conical centrifuge tubes and centrifuged at 3,500g for 20 min. The supernatant was transferred to acid-washed and ultra-pure water-rinsed 15 ml conical centrifuge tubes and spun for an additional 20 min at 4,500g to pellet fine particulates. The clean supernatant from the 15 ml centrifuge tube was transferred to an acid-washed and ultra-pure water-rinsed glass vial. The supernatant was diluted (1:10) to a final volume of 5 ml with ultra-pure water for colorimetric analysis<sup>48</sup>.

Particulate organic carbon and nitrogen values were determined with an elemental analyser as described in ref. 1. Acetate, formate and oxalate concentrations were determined using ion chromatography, following methods in ref. 14.

**Molecular analyses.** DNA was extracted using a modular method to allow for optimization of the DNA extraction procedure, specific to the SLW sediments<sup>49</sup>. DNA extraction yield from SLW sediments was greatest when sediments were pre-treated with 450 μmol g<sup>-1</sup> deoxynucleotide triphosphate to prevent adsorption of lysed DNA to the abundant clay particles in SLW<sup>49</sup>. The particulate methane monooxygenase (*pmoA*) gene clone libraries were constructed by Polymerase Chain Reaction (PCR) amplification using A189F (5'-GGNGACTGG GACTTCTGG-3') and m680R (5'-CCGGMGCAACGTCYTTACC-3')<sup>24</sup>. The PCR was set up using 0.13 μl of ExTaq at 5 units μl<sup>-1</sup> (Takara), 2.5 μl of 10× ExTaq buffer (Takara), 2 μl dNTP mixture at 2.5 mM per nucleotide (Takara), 2.5 μl of A189F and Mb661R primers (10 pmol μl<sup>-1</sup>), 2 μl molecular biology-grade bovine serum albumen (BSA; 1.6 mg ml<sup>-1</sup> final concentration) (New England BioLabs), 4 μl of template DNA (0.01–0.09 ng DNA μl<sup>-1</sup>), and 11.37 μl of PCR-grade water for a final reaction volume of 25 μl. The PCR thermocycling conditions were 1 cycle of 98 °C for 2 min; 40 cycles of 98 °C for 15 s, 55 °C for 1 min, and 72 °C for 1 min; followed by a final 72 °C for 7 min. PCR was conducted with DNA extraction blanks and no template blanks (PCR-grade water) as negative controls. Negative controls were not carried forward for cloning, as no PCR bands were detected. PCR products were run on a 1.5% agarose gel and the 491 basepair *pmoA* fragment was excised from the gel with sterile razor blade and DNA was purified using a Wizard SV gel clean-up system (Promega). Cleaned *pmoA* fragments were immediately ligated and cloned with a TA Cloning kit (Invitrogen). Positive clones were transferred to LB+ampicillin broth and grown overnight at 37 °C, then sequenced (288 total sequenced clones) (Functional Bioscience). The *pmoA* DNA sequences were processed by removing the forward and reverse primer sequences and removing poor-quality sequences (<20 phred score)<sup>50</sup>. Quality controlled *pmoA* sequences (176 total) were clustered into operational taxonomic units (OTUs) at the 97% similarity level and one representative sequence from each OTU<sup>51</sup>, along with representative *pmoA* sequences from type Ia and II methanotrophs<sup>24</sup>, were aligned using ClustalW using the default alignment parameters within the program MEGA6 (ref. 52). A phylogenetic tree was built using the neighbour-joining method with 1,000 bootstrap replications<sup>52</sup>. The *pmoA* sequences have been deposited in GenBank under accession numbers KX589304–KX589461 and KX784213–KX84230.

We attempted to amplify *mcrA* gene sequences from SLW sediment DNA extracts using a primer set designed to amplify the diversity of *mcrA*-containing methanogens<sup>18</sup> with a nested PCR amplification scheme. The primer pair used to detect the *mcrA* gene sequence were *mcrIRD*<sup>18</sup>. The primer pair is capable of detecting a wide diversity of known and several novel *mcrA* gene clusters<sup>18</sup>. The first reaction was set up using 0.13 μl of Takara ExTaq at 5 units μl<sup>-1</sup>, 2.5 μl 10× ExTaq buffer, 2 μl dNTP mixture at 2.5 mM per nucleotide (Takara), 2.5 μl of forward and reverse primer (10 pmol μl<sup>-1</sup>), 2 μl of BSA (1.6 mg ml<sup>-1</sup> final concentration), 9.38 μl PCR-grade water and 4 μl DNA extract (0.01–0.09 ng DNA μl<sup>-1</sup>) for a final reaction volume of 25 μl. This first reaction was with an initial denaturation step at 98 °C for 2 min followed by 40 cycles of 98 °C for 15 s, 53 °C for 1 min and 72 °C for 1 min, and a final elongation at 72 °C for 7 min. The second reaction was set up using 0.25 μl Takara ExTaq, 5 μl 10× ExTaq buffer, 4 μl dNTP mixture at 2.5 mM per nucleotide (Takara), 5 μl of forward and reverse primers (10 pmol μl<sup>-1</sup>), 4 μl of BSA (1.6 mg ml<sup>-1</sup> final concentration), 21.75 μl of

PCR-grade water and 4 µl of product from the first reaction as template DNA. The second reaction was run with the same thermocycler program as the first reaction. PCR was conducted with DNA extraction blanks and no template blanks (PCR-grade water) as negative controls. Details of the 16S rRNA molecule sample collection and preservation, extraction, reverse transcription, sequencing and processing are described in ref. 21. Extraction blanks were conducted, processed and analysed in parallel with the SLW sediment samples as described in ref. 21.

**Chemical affinity calculations.** An assessment of CH<sub>4</sub> as a potential chemical energy source for the surficial (0–2 cm) sediment layer was undertaken. The chemical affinity of coupled oxidation–reduction reactions involving CH<sub>4</sub> and other potential metabolic reactions was determined. The chemical affinity ( $A_r$ ) is the maximum amount of energy that can be obtained for a reaction based on *in situ* conditions.  $A_r$  is defined as the change in the overall Gibbs energy under non-equilibrium conditions ( $\Delta G_r^\circ$ ) with a change in the progress of the reaction, which quantifies the reactions proximity to equilibrium<sup>30,31</sup> and is given by:

$$A_r = RT \ln(K_r/Q_r) \quad (3)$$

where  $K_r$  is the calculated equilibrium constant for the reaction, which is derived from  $\Delta G_r^\circ$  of the reaction according to  $\Delta G_r^\circ = G_r^\circ \text{ products} - G_r^\circ \text{ reactants}$ , where  $G_r^\circ$  is the standard Gibbs energy of formation for the products and reactants<sup>53</sup>.  $K_r$  is given by:

$$K_r = e^{-\Delta G_r^\circ/RT} \quad (4)$$

where  $R$  is the gas constant 0.008314 kJ mol<sup>-1</sup>, and  $T$  is SLW temperature in Kelvin [ $-0.5^\circ\text{C} = 272.65\text{K}$ ] (ref. 53). Thermodynamic values were derived from ref. 31 using values for 2 °C, the closest available values for the temperature of SLW ( $-0.5^\circ\text{C}$ ); the impact of the temperature difference on  $\Delta G_r^\circ$  and resulting  $K_r$  values will be small<sup>30,31</sup>.

$Q_r$  is the activity product for the reaction, determined as;

$$Q_r = \prod_i (a_i)^{\nu_{i,r}} \quad (5)$$

where  $a_i$  represents the activity of the  $i$ th compound in the reaction raised to its stoichiometric coefficient in the  $r$ th reaction,  $\nu_{i,r}$ , which is positive for products and negative for reactants. Activities are calculated from molal concentrations ( $m_i$ ) using activity coefficients ( $\gamma_i$ ) and the relationship  $a_i = m_i \gamma_i$  (ref. 30). These activities were calculated using the geochemical model PHREEQC<sup>54</sup> using the empirical SLW geochemistry<sup>7,14</sup>. The O<sub>2</sub> concentration in the 0–2 cm layer was not measured, but for the chemical affinity calculations we consider two scenarios of O<sub>2</sub> concentration set at 50% (36.5 µM) and 10% (7.3 µM) of average SLW lake water to account for the decrease in sedimentary O<sub>2</sub> concentration due to consumption and diffusion<sup>55</sup>. Given that oxygen is inferred to penetrate to ~16 cm based on redox-sensitive trace metal concentrations<sup>14</sup>, it is reasonable to model chemical affinity using these two concentrations of O<sub>2</sub> in the surficial sediment. Temperature, pH, redox (pE) and concentrations of acetate, formate (Supplementary Fig. 1), dissolved inorganic carbon (DIC), O<sub>2</sub> (aq), CH<sub>4</sub> (aq), SO<sub>4</sub><sup>2-</sup>, NO<sub>3</sub><sup>-</sup>, NH<sub>4</sub><sup>+</sup>, total dissolved Fe, Ca<sup>2+</sup>, Mg<sup>2+</sup>, Na<sup>+</sup>, K<sup>+</sup>, P, Li<sup>+</sup>, Br<sup>-</sup>, Cl<sup>-</sup> and F<sup>-</sup> were defined<sup>7,14,32,47</sup>. Redox-sensitive elements that were measured as total dissolved elemental concentration (that is, C, Fe) were assumed to be speciated to the redox states and species activities as determined by PHREEQC. Conversely, ions measured in specific redox states (that is, SO<sub>4</sub><sup>2-</sup>, NO<sub>3</sub><sup>-</sup>, NH<sub>4</sub><sup>+</sup>) were maintained in their respective redox states by the model, and the species activities including these ions were calculated.

The chemical affinities are expressed in per electron yields ( $A_r^{e^-}$ ) and also shown in terms of energy density, the energy per kg H<sub>2</sub>O ( $A_r^{kg}$ ), which scales the energy availability to the limiting reactant, calculated as:

$$A_r^{kg} = \left| \frac{A_r}{\nu_i} \right| [i] \quad (6)$$

where  $[i]$  refers to the concentration of the limiting electron donor or acceptor<sup>56</sup>. This scaling (equation (6)) of chemical affinity has been shown to better correlate with actual microbial communities and metabolisms than the chemical affinity normalized to moles of electrons transferred<sup>56,57</sup>.

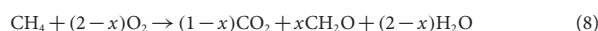
**Methane oxidation rate modelling.** CH<sub>4</sub> oxidation rates were modelled by calculating the flux of CH<sub>4</sub> into the 0–2 cm sediment layer. The CH<sub>4</sub> concentration gradient was determined using CH<sub>4</sub> values from 15 cm to 3 cm. The flux was calculated using Fick's first law and the error of the flux determined from the error associated with the diffusional gradient. Water content was measured and calculated by weighing a known volume of wet weight sediment, then measuring the sediment again after drying at 95 °C for three days<sup>43,45</sup>. Porosity was calculated from the water content and density of the sediment<sup>43,45</sup>. The diffusion coefficient

for CH<sub>4</sub> at 0 °C was corrected for porosity (Supplementary Fig. 3) and tortuosity of SLW sediments calculated according to equation (3.11) from ref. 58 with  $C = 2.02$  (refs 58,59). We modelled the rate of biological CH<sub>4</sub> consumption according to equation (1) (see main text).

The control volume of our model can be defined by the relationship:

$$V = A \times H_L + (H_{SS} \times \varphi) \quad (7)$$

where  $H_L$  and  $H_{SS}$  are the height of the lake and surficial sediments, respectively, and  $\varphi$  is the sediment porosity. Assuming steady-state conditions (that is,  $dC/dt = 0$ ) and substitution of equation (7) into equation (1),  $R$  can be calculated as shown in equation (2).  $R$  represents the sum of both microbial CH<sub>4</sub> oxidation to CO<sub>2</sub> and incorporation of CH<sub>4</sub> into biomass. We estimated the amount of CH<sub>4</sub> removal due to oxidation and incorporation of biomass by assuming that the biomass partitioning factor of CH<sub>4</sub> going to biomass is 0.5 ( $x$ ; equation (8)). The value of 0.5 has been shown to be a good approximation for the fraction of biomass incorporated by type I methanotrophs during CH<sub>4</sub> oxidation and is a median value across many habitats<sup>33,60,61</sup>. We calculated the impact of varying  $x$  from 0.06 to 0.77 (ref. 36) on biomass C production and methanotrophy oxygen demand (Supplementary Table 1). From the CH<sub>4</sub> removal rate and the fraction of CH<sub>4</sub> incorporated into biomass, we can then calculate the O<sub>2</sub> consumption by CH<sub>4</sub> oxidation, which follows the stoichiometric relationship:



where  $x$  is the fraction of CH<sub>4</sub> partitioned into biomass formation<sup>33,60,62</sup>. The inputs of O<sub>2</sub> to the lake are from atmospheric gases released by melting of the overlying meteoric ice and advection of water into the lake during the filling phase of the hydrologic cycle<sup>9,32,63</sup>. Based on the concentration of gas in the overlying ice and the basal ice melt rate, which has been estimated at 1.8 cm yr<sup>-1</sup> (ref. 9), the overlying ice sheet supplies  $1.0 \times 10^6$  mol O<sub>2</sub> yr<sup>-1</sup> (67% of O<sub>2</sub> supply to SLW)<sup>32</sup>. Advection into the lake provides  $5 \times 10^5$  mol O<sub>2</sub> yr<sup>-1</sup> (33% of O<sub>2</sub> supply to SLW)<sup>32</sup>, assuming the incoming water has the same concentration measured in the SLW water column<sup>32,63</sup>. When the fraction of carbon from CH<sub>4</sub> going to biomass is varied (Supplementary Table 1), the oxygen demand on the system changes as well. We used the SLW oxygen budget from ref. 32 to determine the impact the biomass partitioning factor ( $x$ ) could have on the oxygen demand for biological processes in SLW (Supplementary Table 1).

**Data availability.** Data generated for this study are available through the Microbial Antarctic Resource System database (<http://mars.biodiversity.aq/resources/97>). Molecular data were accessed from NCBI Sequence Read Archive (<https://www.ncbi.nlm.nih.gov/sra>) project PRJNA244335.

## References

- Priscu, J. C. *et al.* A microbiologically clean strategy for access to the Whillans Ice Stream subglacial environment. *Antarct. Sci.* **11**, 1–11 (2013).
- Tulaczyk, S. *et al.* WISSARD at Subglacial Lake Whillans, West Antarctica: scientific operations and initial observations. *Ann. Glaciol.* **55**, 51–58 (2014).
- National Resource Council *Exploration of Antarctic Subglacial Aquatic Environments* (The National Academies Press, 2007).
- Riedinger, N. *et al.* Methane at the sediment–water transition in Black Sea sediments. *Chem. Geol.* **274**, 29–37 (2010).
- Wiesenburg, D. A. & Guinasso, N. L. Jr Equilibrium solubilities of methane, carbon monoxide, and hydrogen in water and sea water. *J. Chem. Eng. Data* **24**, 356–360 (1979).
- Avnimelech, Y., Ritvo, G., Meijer, L. E. & Kochba, M. Water content, organic carbon and dry bulk density in flooded sediments. *Aquacult. Eng.* **25**, 25–33 (2001).
- Yarnes, C. <sup>13</sup>C and <sup>2</sup>H measurement of methane from ecological and geological sources by gas chromatography/combustion/pyrolysis isotope-ratio mass spectrometry. *Rapid Commun. Mass Spectrom.* **27**, 1036–1044 (2013).
- Vick-Majors, T. J. *Biogeochemical Processes in Antarctic Aquatic Environments: Linkages and Limitations* (Montana State University, 2016).
- Solorzano, L. Determination of ammonia in natural waters by the phenylhypochlorite method. *Limnol. Oceanogr.* **14**, 799–801 (1969).
- Lever, M. A. *et al.* A modular method for the extraction of DNA and RNA, and the separation of DNA pools from diverse environmental sample types. *Front. Microbiol.* **6**, 476 (2015).
- Paegel, B. M., Emrich, C. A., Wedemayer, G. J., Scherer, J. R. & Mathies, R. A. High throughput DNA sequencing with a microfabricated 96-lane capillary array electrophoresis bioprocessor. *Proc. Natl Acad. Sci. USA* **99**, 574–579 (2002).
- Schloss, P. D. *et al.* Introducing mothur: open-source, platform-independent, community-supported software for describing and comparing microbial communities. *Appl. Environ. Microbiol.* **75**, 7537–7541 (2009).

52. Tamura, K., Stecher, G., Peterson, D., Filipski, A. & Kumar, S. MEGA6: molecular evolutionary genetics analysis version 6.0. *Mol. Biol. Evol.* **30**, 2725–2729 (2013).
53. Stumm, W. & Morgan, J. J. *Aquatic Chemistry: Chemical Equilibria and Rates in Natural Waters* (Wiley-Interscience, 1996).
54. Parkhurst, D. L. & Appelo, C. A. J. *US Geological Survey Techniques and Methods* 497 (US Geological Survey, 2013).
55. Boetius, A. & Wenzhöfer, F. Seafloor oxygen consumption fuelled by methane from cold seeps. *Nat. Geosci.* **6**, 725–734 (2013).
56. LaRowe, D. E. & Amend, J. P. in *Microbial Life of the Deep Biosphere* (eds Kallmeyer, J. & Wagner, D.) 279–302 (Walter de Gruyter, 2014).
57. Osburn, M. R. *et al.* Chemolithotrophy in the continental deep subsurface: Sanford Underground Research Facility (SURF), USA. *Front. Microbiol.* **5**, 610 (2014).
58. Shen, L. & Chen, Z. Critical review of the impact of tortuosity on diffusion. *Chem. Eng. Sci.* **62**, 3748–3755 (2007).
59. Broecker, W. S. & Peng, T.-H. Gas exchange rates between air and sea. *Tellus* **26**, 21–35 (1974).
60. Shelley, F., Abdullahi, F., Grey, J. & Trimmer, M. Microbial methane cycling in the bed of a chalk river: oxidation has the potential to match methanogenesis enhanced by warming. *Freshw. Biol.* **60**, 150–160 (2015).
61. Whalen, S. C., Reeburgh, W. S. & Sandbeck, K. A. Rapid methane oxidation in a landfill cover soil. *Appl. Environ. Microbiol.* **56**, 3405–3411 (1990).
62. Urmann, K., Lazzaro, A., Gandolfi, I., Schroth, M. H. & Zeyer, J. Response of methanotrophic activity and community structure to temperature changes in a diffusive CH<sub>4</sub>/O<sub>2</sub> counter gradient in an unsaturated porous medium. *FEMS Microbiol. Ecol.* **69**, 202–212 (2009).
63. Siegfried, M. R., Fricker, H. A., Carter, S. P. & Tulaczyk, S. Episodic ice velocity fluctuations triggered by a subglacial flood in West Antarctica. *Geophys. Res. Lett.* **43**, 2640–2648 (2016).